



REPM 2025 NIMS
TSUKUBA



TECHNISCHE
UNIVERSITÄT
DARMSTADT

Reduction of heavy rare earths in Nd-Fe-B-based magnets by diffusion source and application area optimization

**Imants Dirba¹, Abdullatif Durgun¹, Dominik Ohmer², Matthias Katter², Andreas Thul³,
Hossein Sepehri Amin⁴, Oliver Gutfleisch¹**

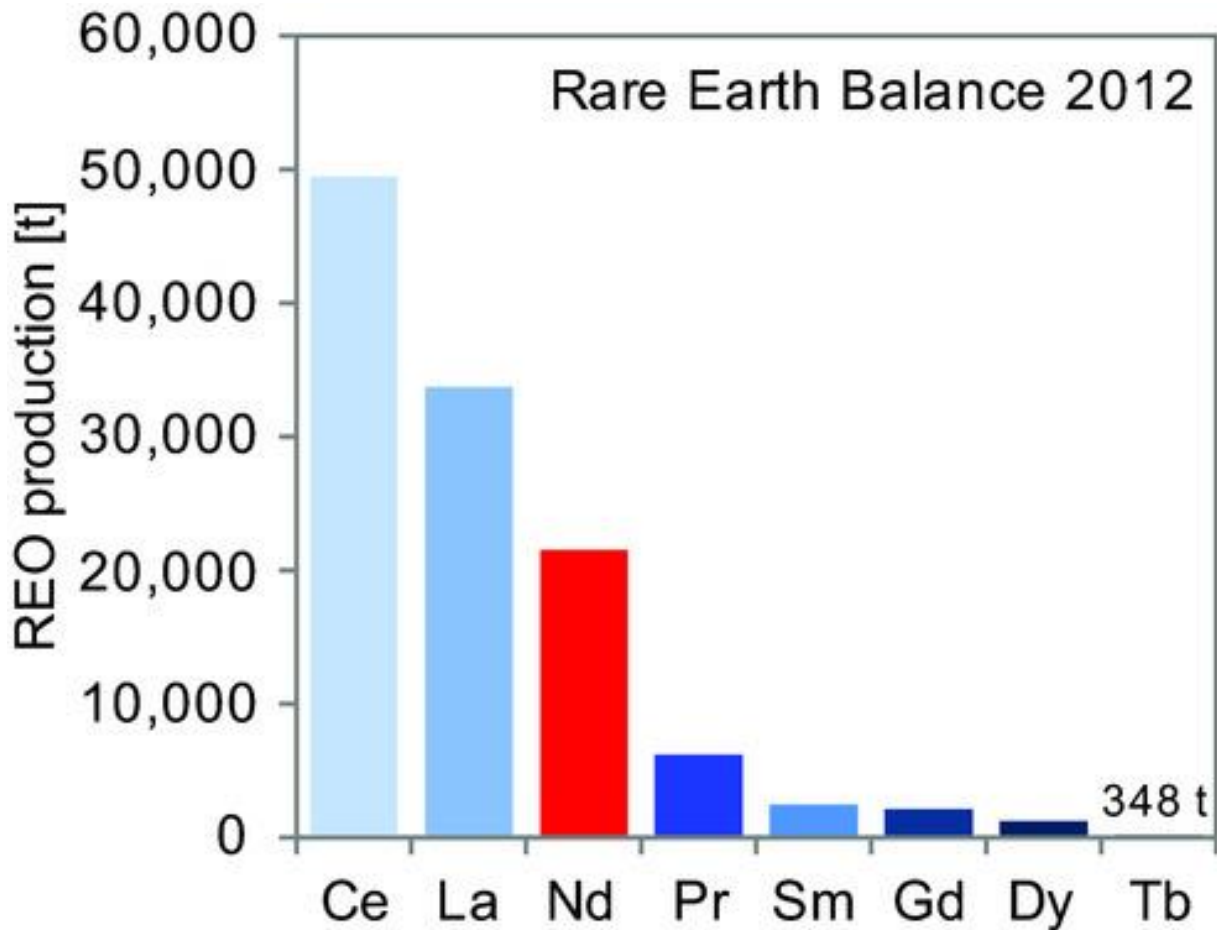
¹Functional Materials, Institute of Materials Science, Technical University of Darmstadt, 64287 Darmstadt, Germany,

²Vacuumschmelze GmbH & Co. KG, 63412 Hanau, Germany, ³Institute of Electrical Machines (IEM),

³RWTH Aachen University, 52062 Aachen, Germany, ⁴National Institute for Materials Science, Tsukuba 305-0047, Japan



What is the best GBDP HRE source?

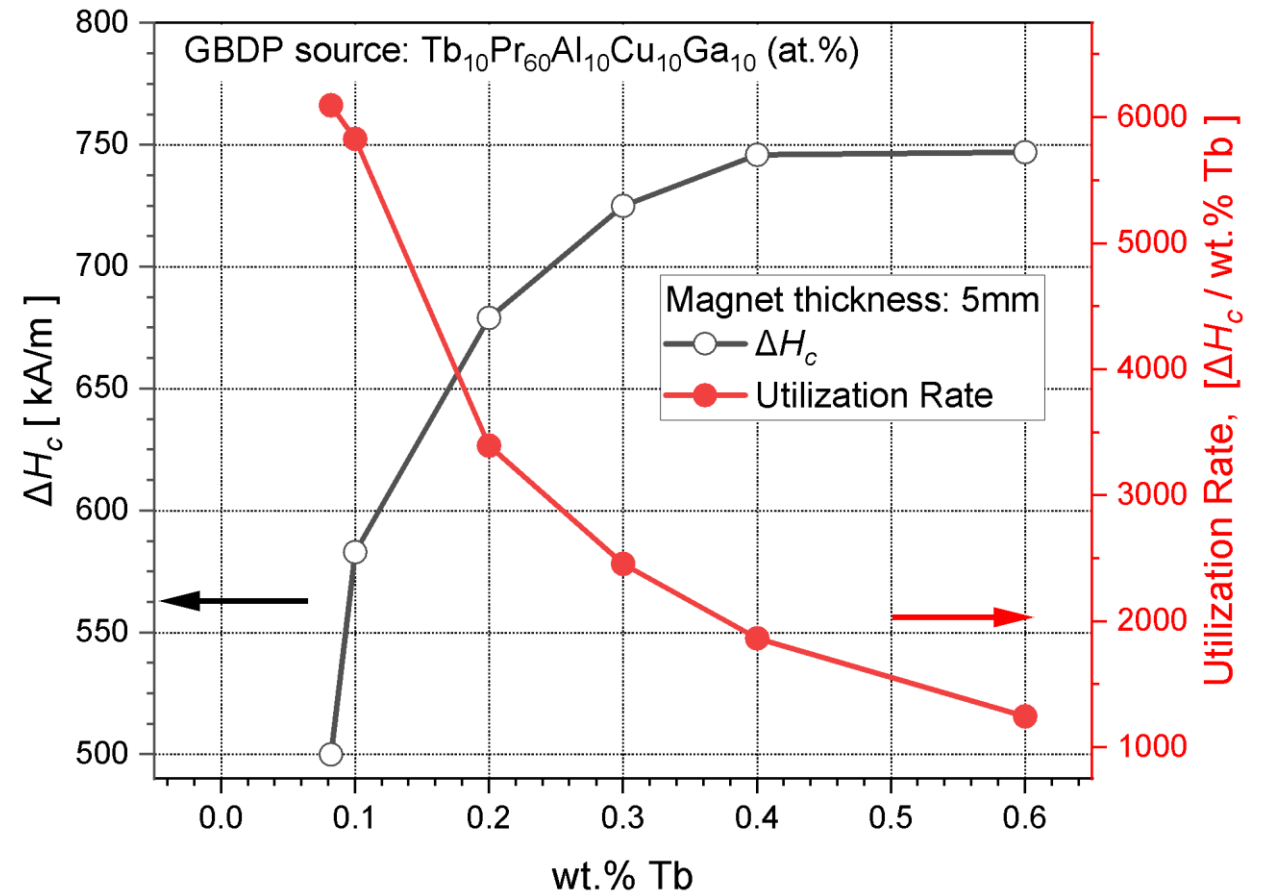
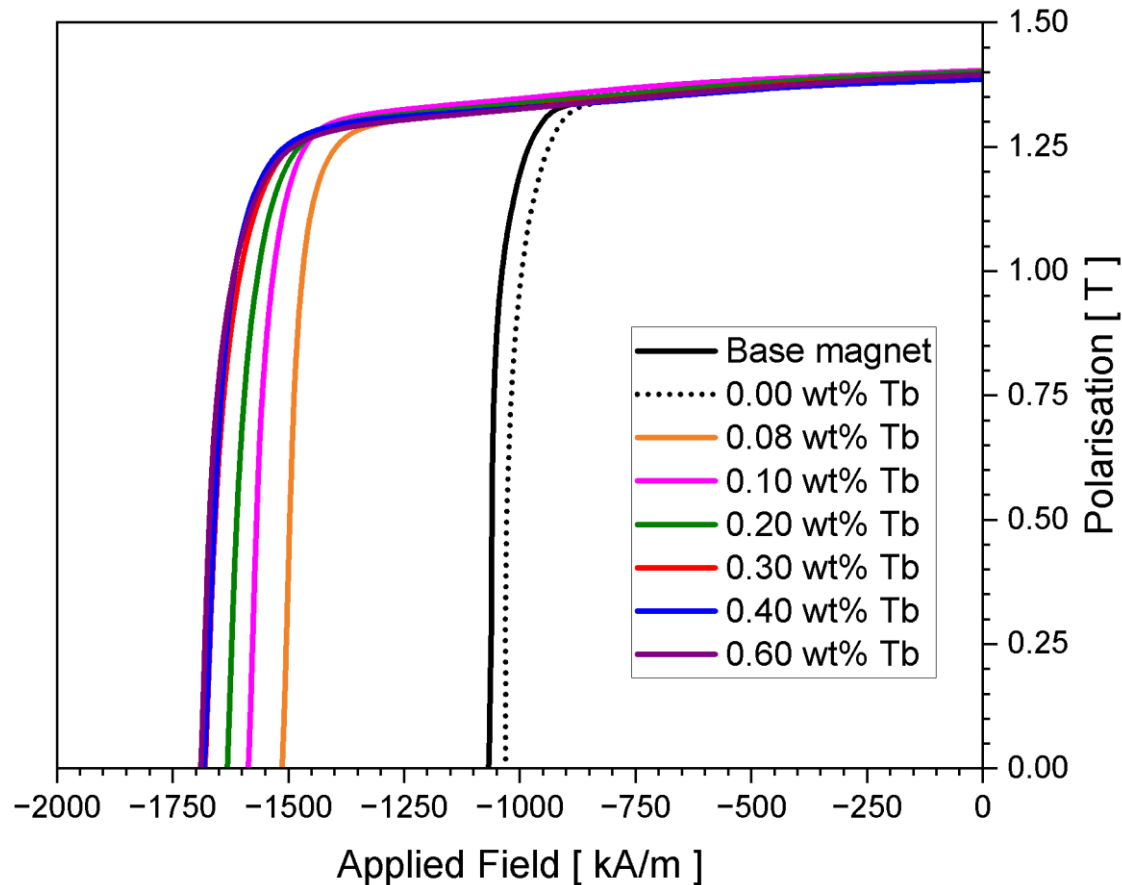


- Rare earth balance: 1 kg of Nd oxide produces 0.02 kg of Tb oxide
- **The highest ΔH_c per HRE amount in the GBDP alloy: complex low-melting alloys $Tb_{10}Pr_{60}(CuAlGa)_{30}$**

Experimental:

- Produced by melt spinning, applied on commercial N50 grade sintered magnets followed by a two-step heat treatment

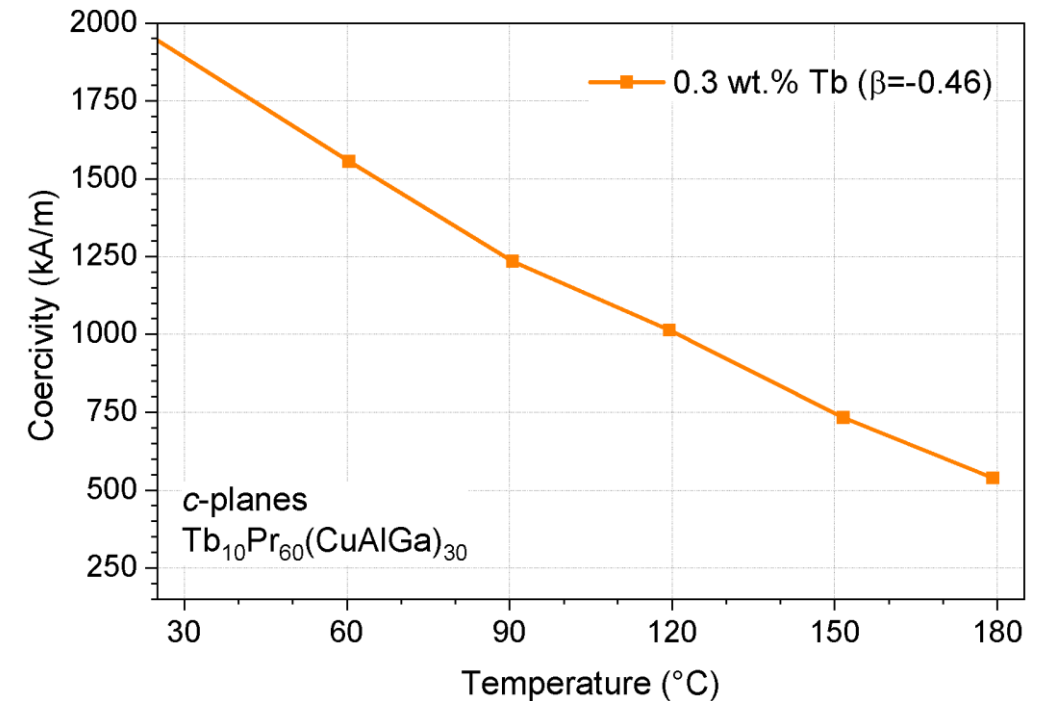
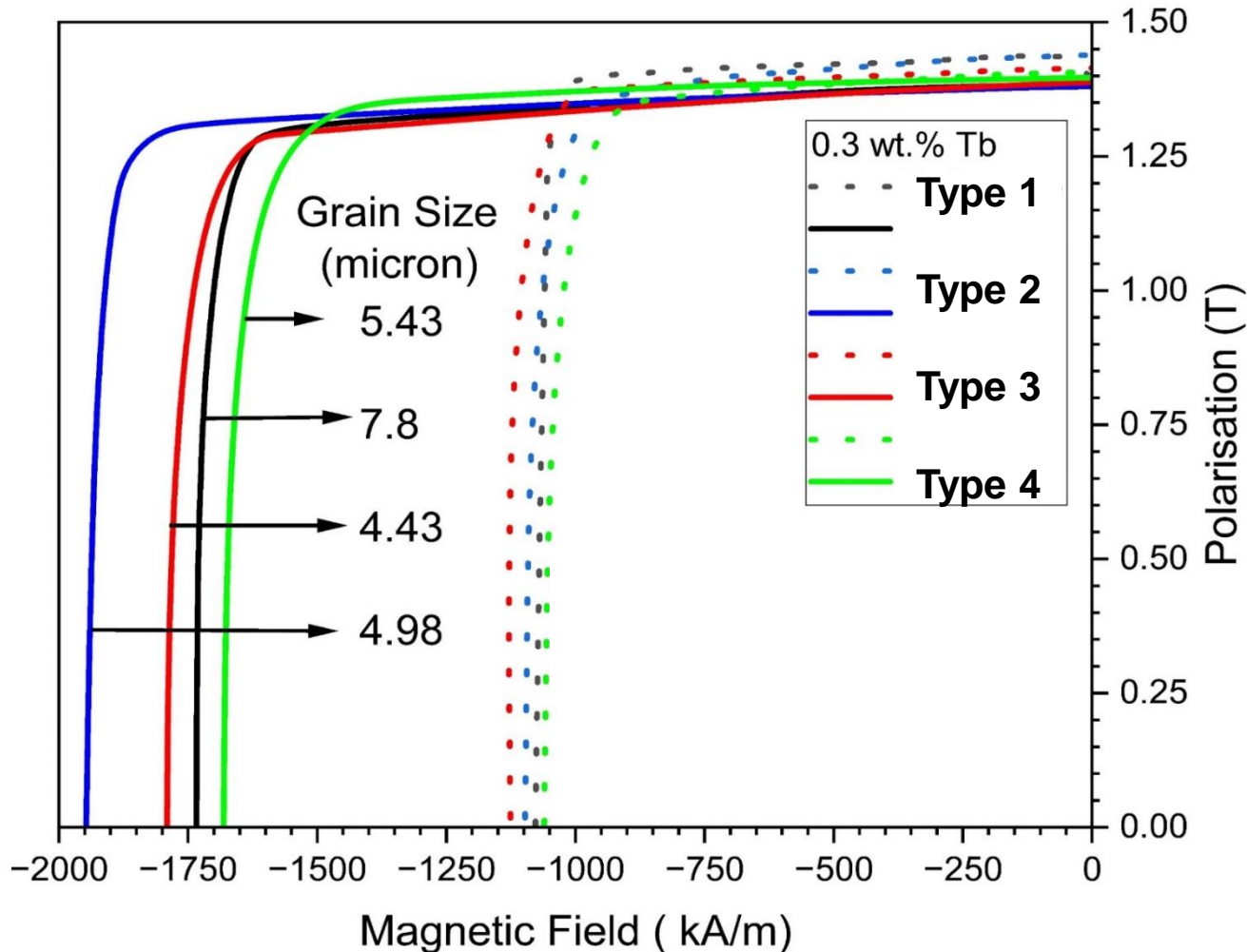
Grain boundary diffusion process optimization



Coercivity enhancement saturates and HRE utilization decreases for high Tb amounts

*Commercial grade VD722HR NdFeB-based sintered magnets from Vacuumschmelze GmbH

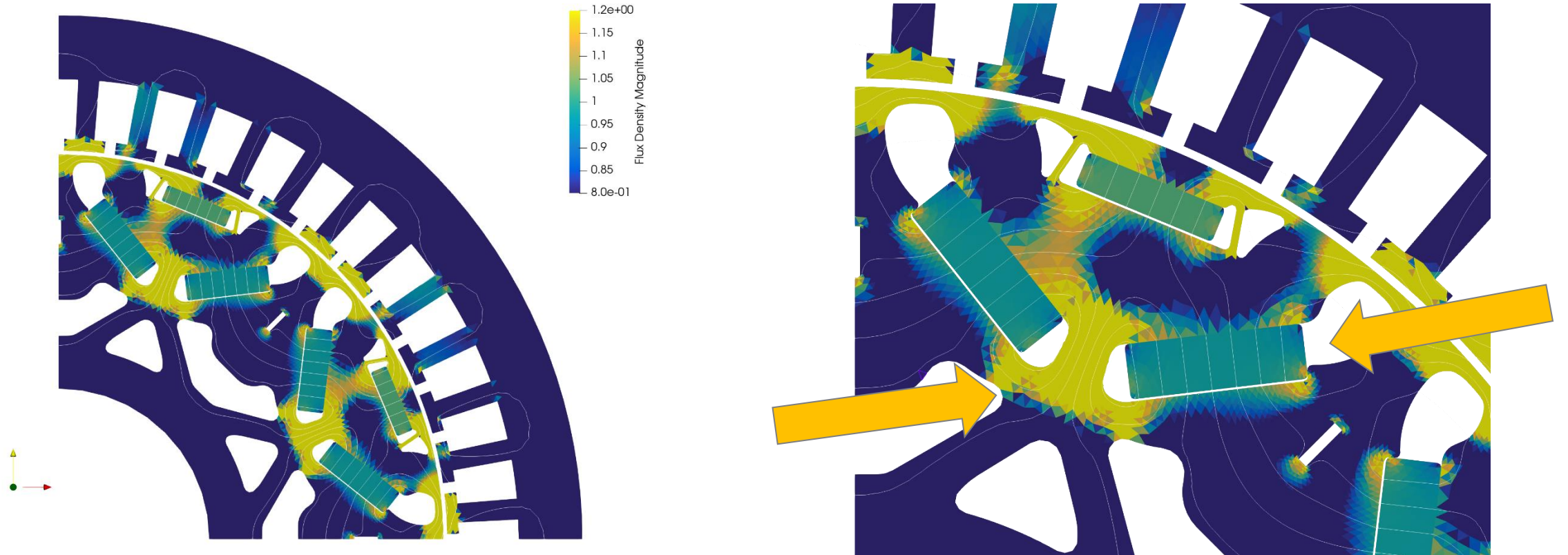
The influence of the initial magnet (N50 grade)



$$J_r = 1.4 \text{ T}, H_c = 1990 \text{ kA/m (2.5 T)}$$

$$H_c = 747 \text{ kA/m (0.94) @ 150 °C}$$

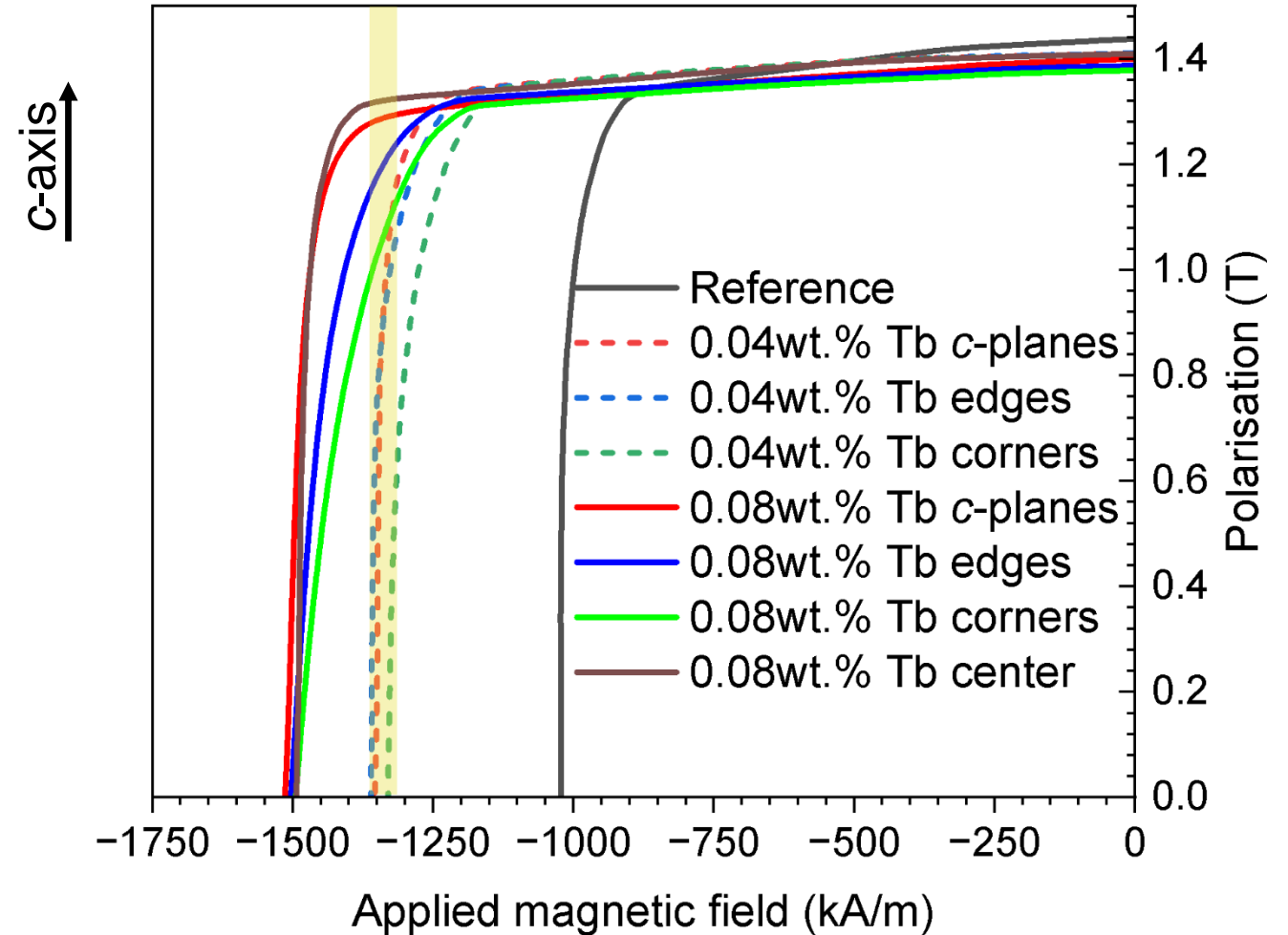
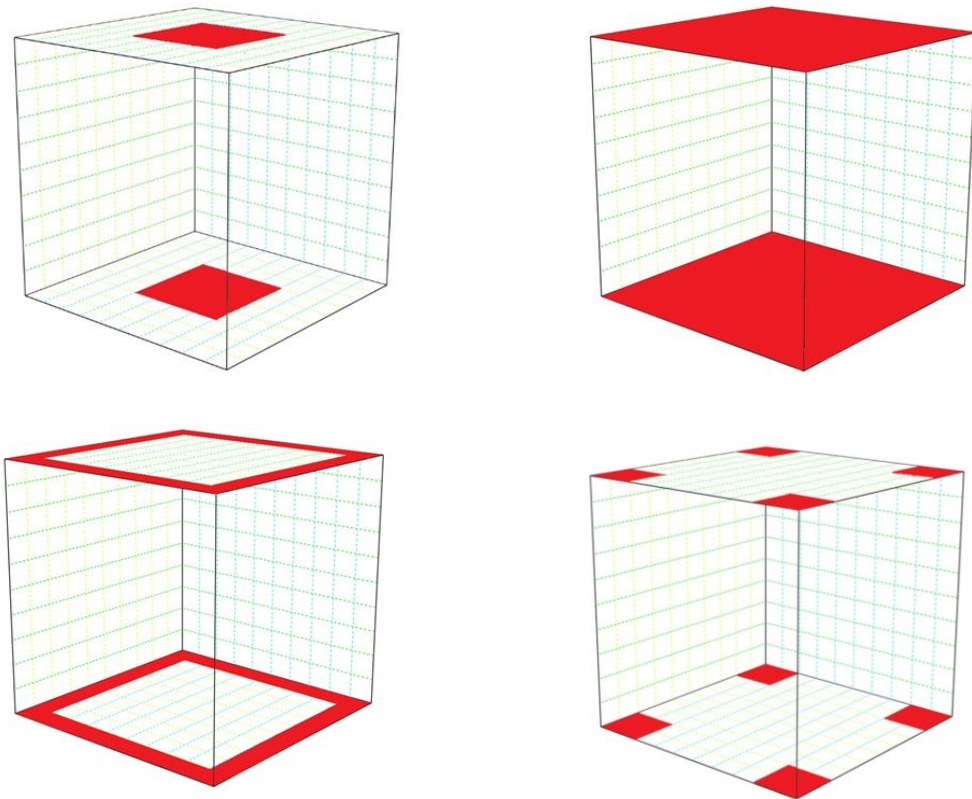
Strategic local magnetic hardening



2D FE-Simulated flux density distribution for a permanent magnet traction motor from electric vehicles

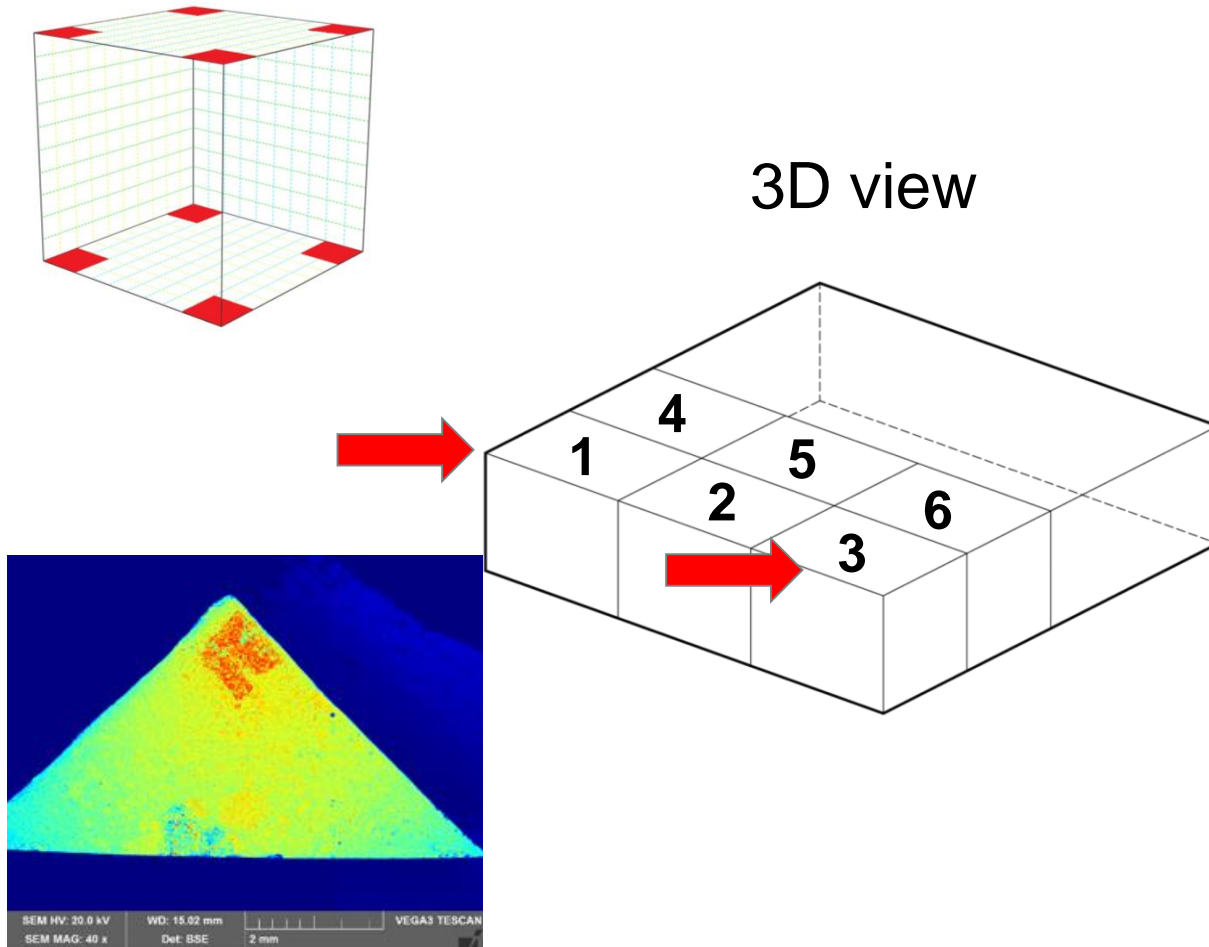
The highest demagnetization at corners/edges. **Local magnetic hardening via selected area GBDP?**

Strategic local magnetic hardening



“3D GBD”, “Gen 3”..

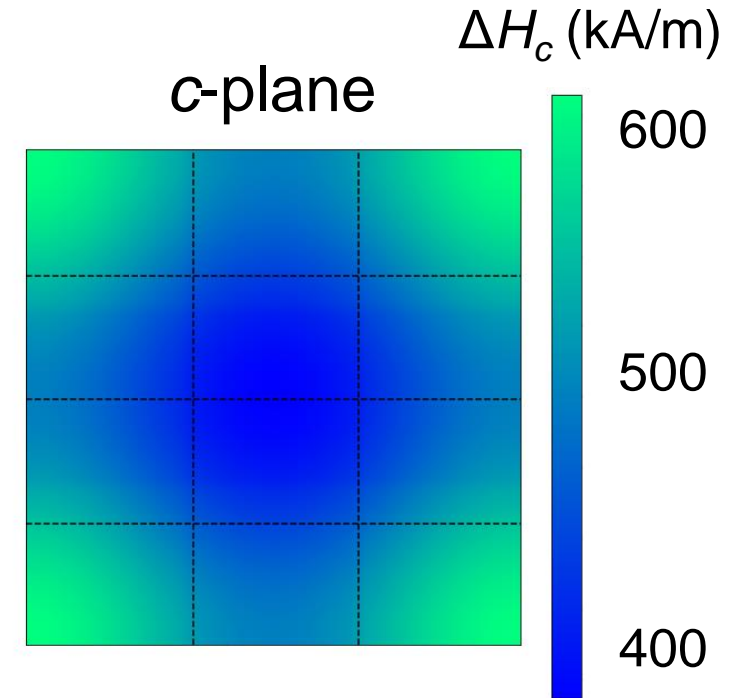
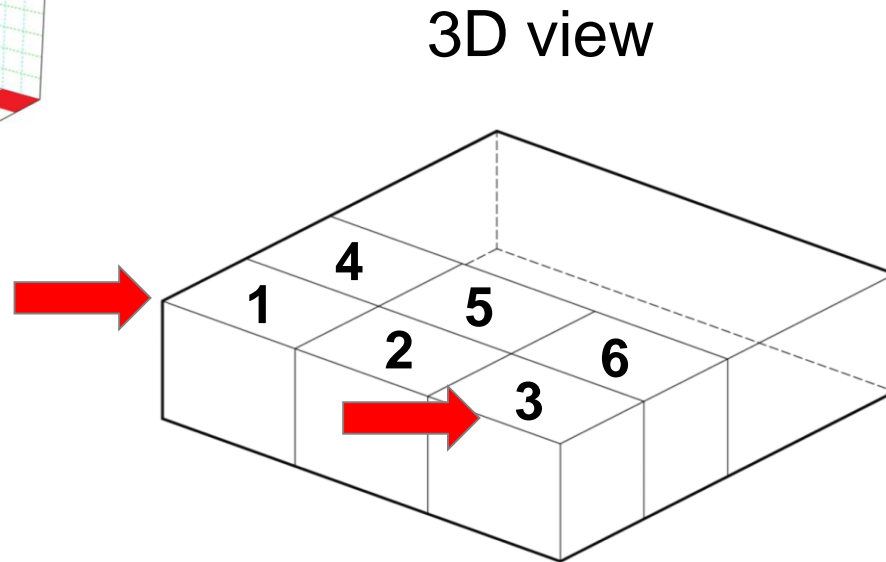
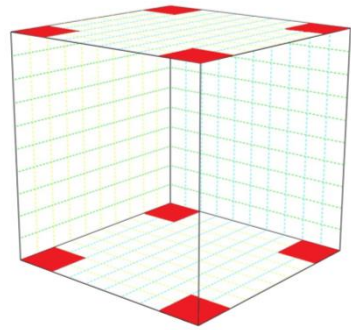
Local magnetic hardening – how to characterize?



| Position | H_c (kA/m) | ΔH_c (kA/m) |
|----------|--------------|---------------------|
| 1 | 1598 | 587 |
| 2 | 1521 | 510 |
| 3 | 1592 | 581 |
| 4 | 1503 | 492 |
| 5 | 1441 | 430 |
| 6 | 1486 | 475 |
| Initial | 1011 | |

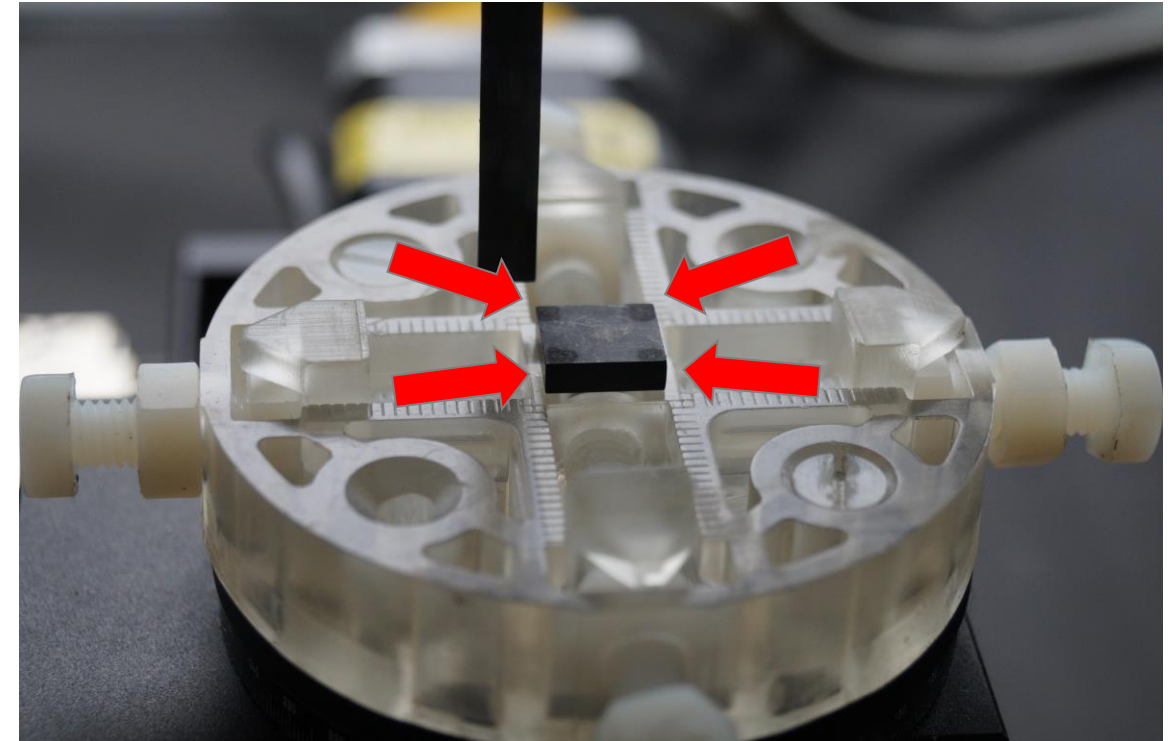
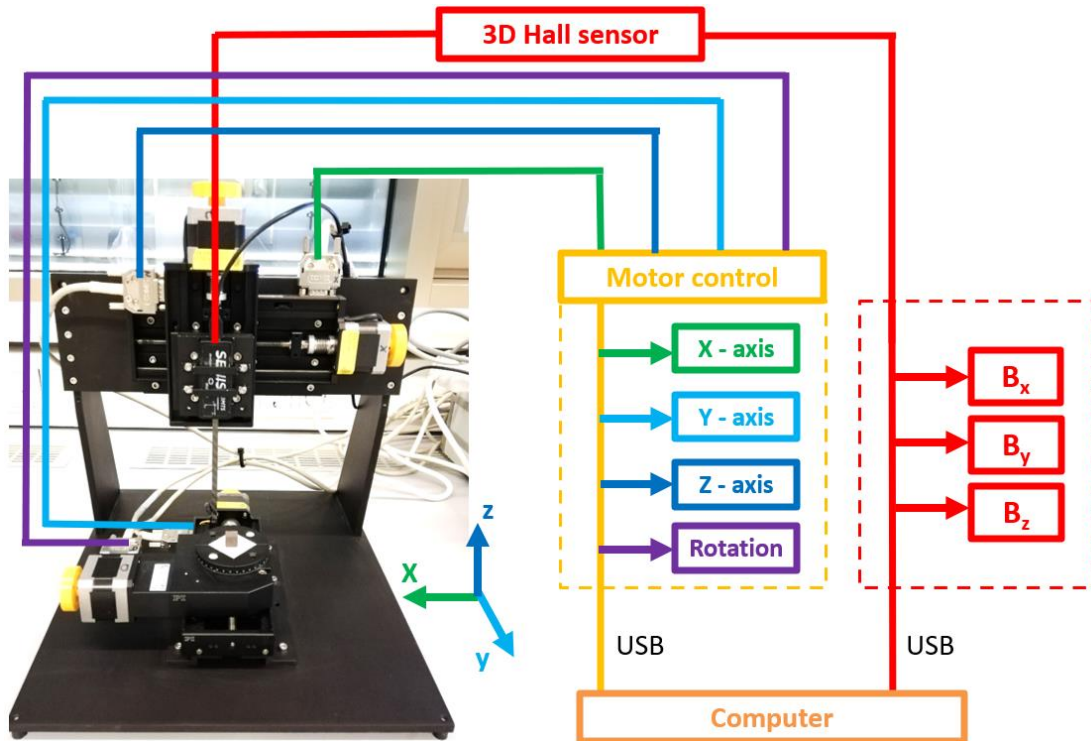
Local coercivity mapping by measuring $M(H)$ each for each individual segment

Local coercivity mapping



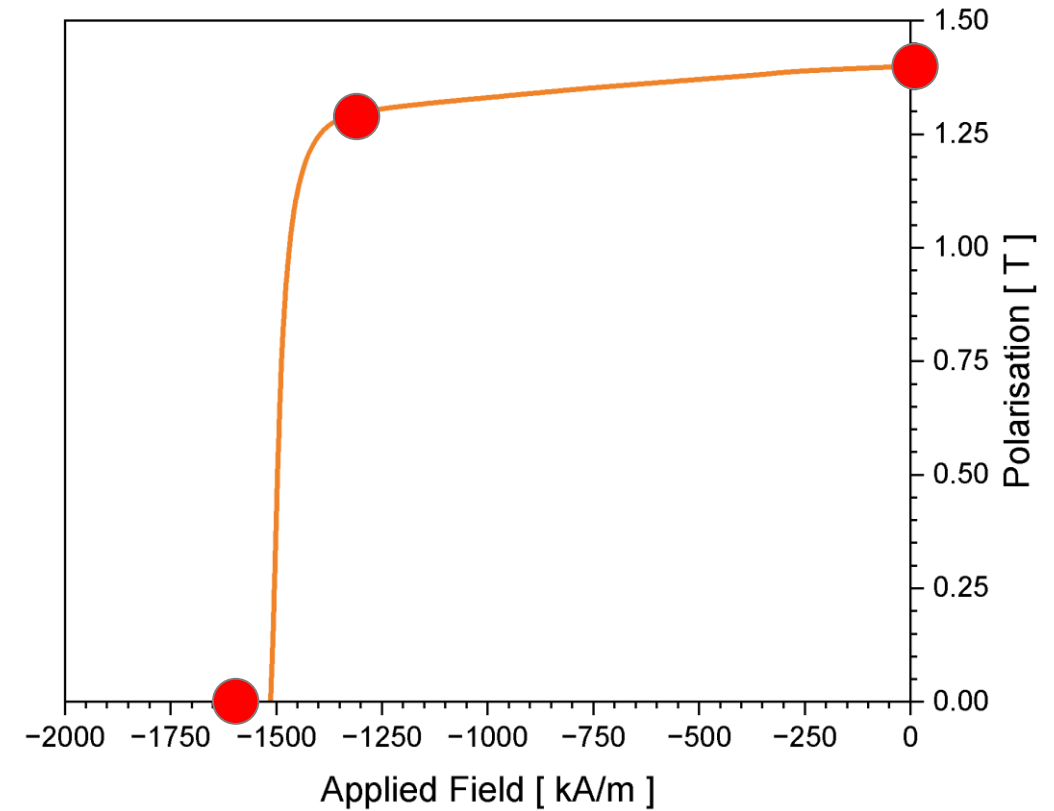
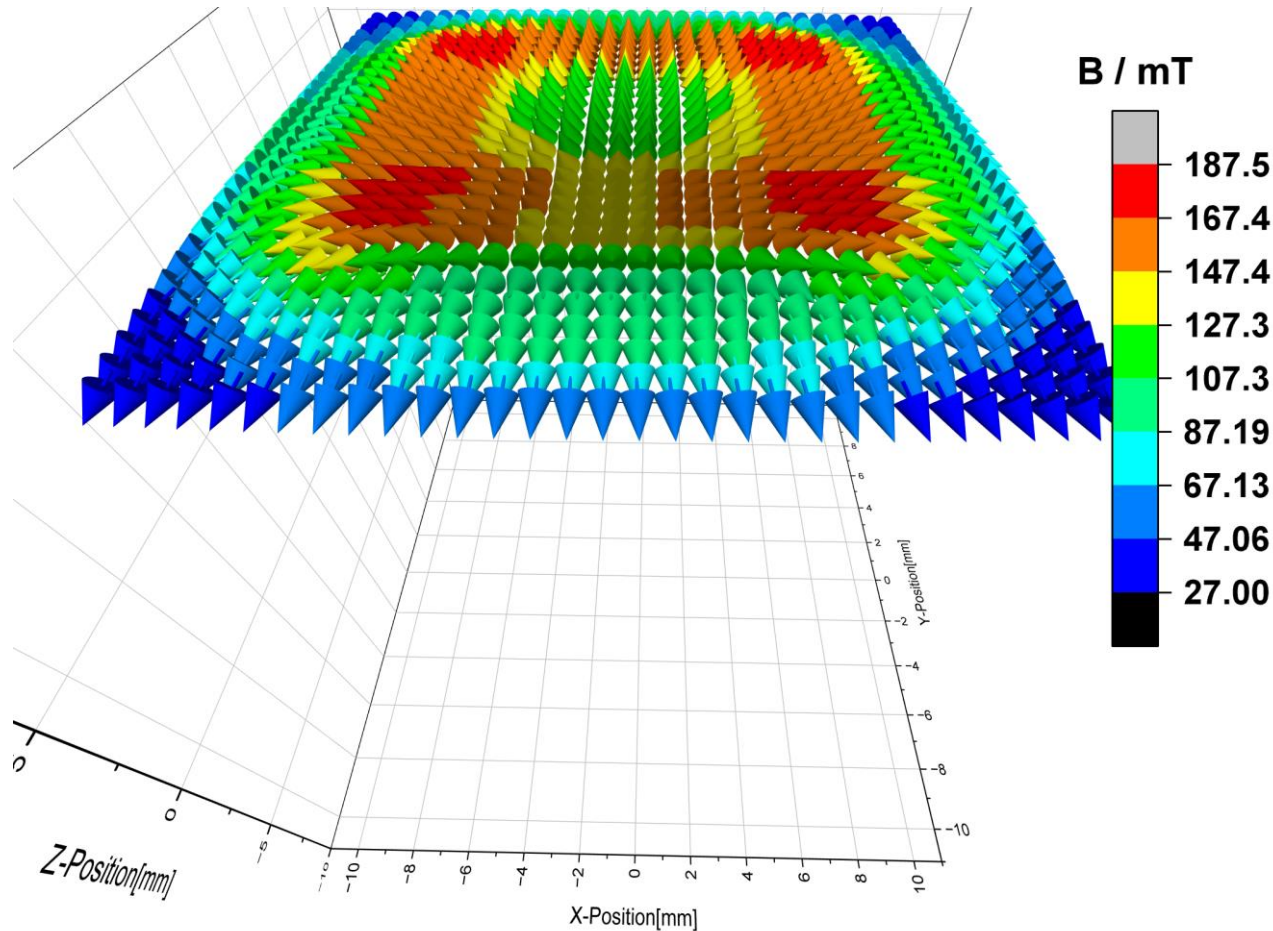
Local coercivity mapping by measuring $M(H)$ each for each individual segment

Strayfield mapping using a 3D hall scanner



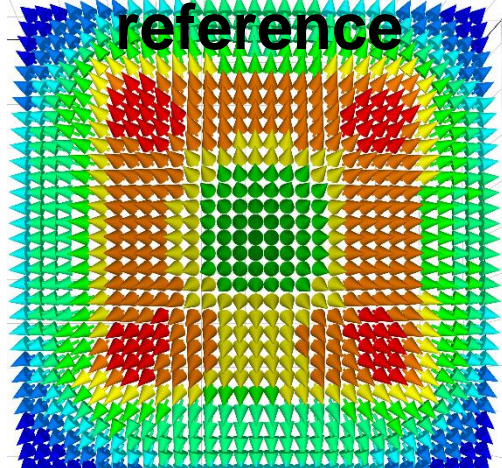
Local mapping of B_x , B_y , B_z above magnet surface across the hysteresis loop

Strayfield mapping using a 3D hall scanner

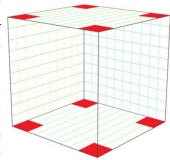
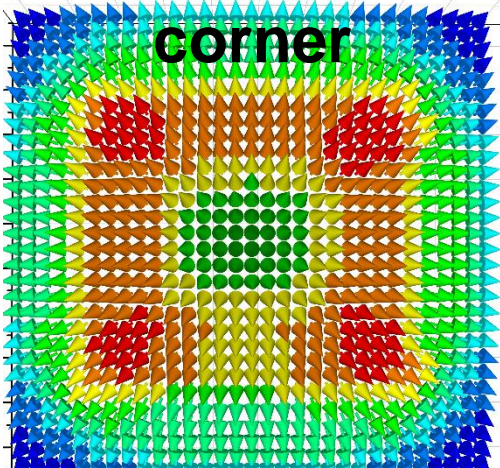


Local mapping of B_z above magnet surface across the hysteresis loop

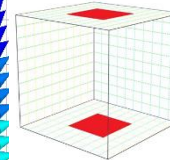
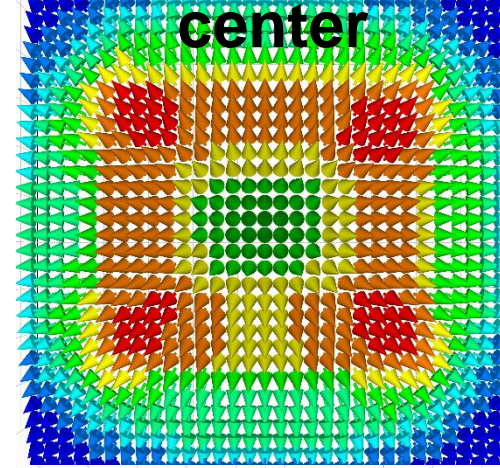
saturated



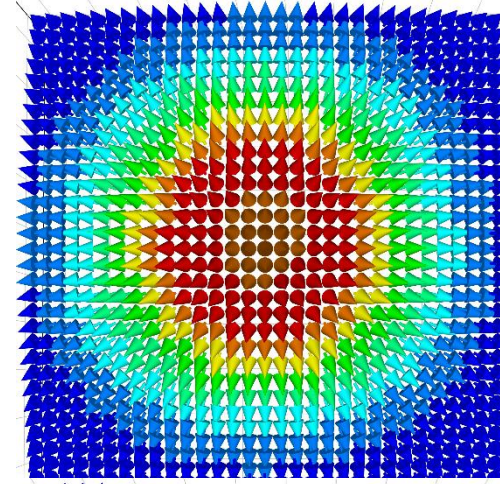
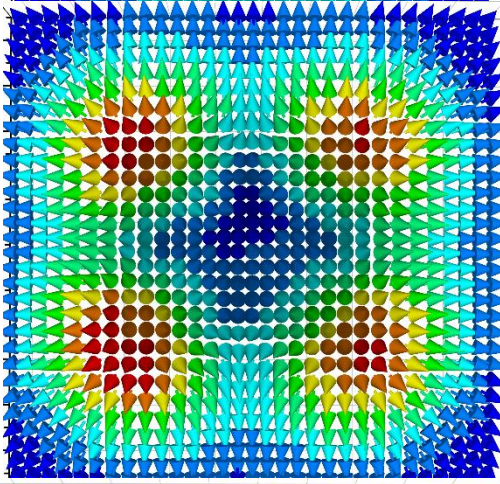
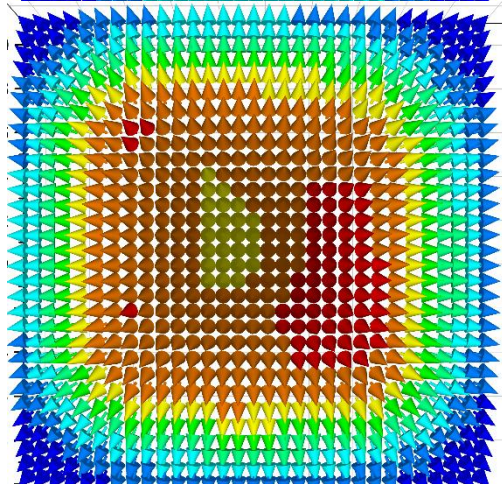
corner



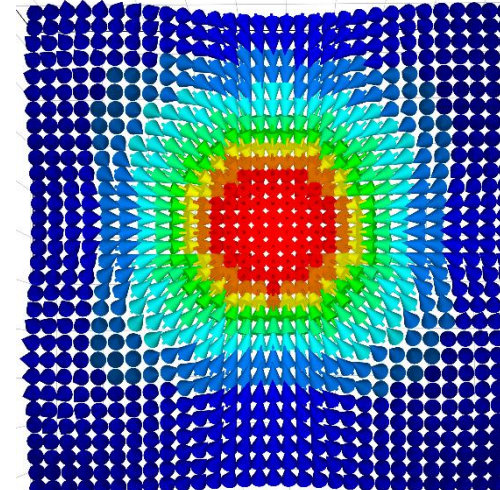
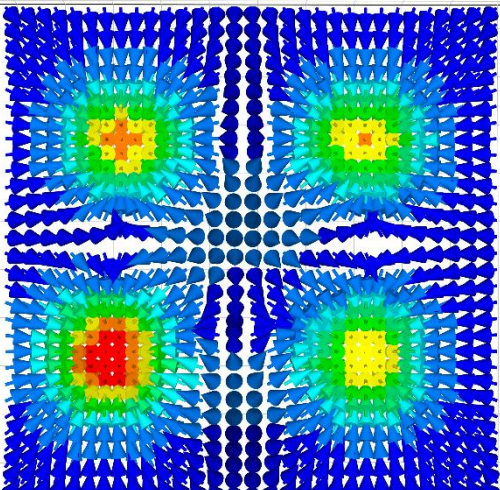
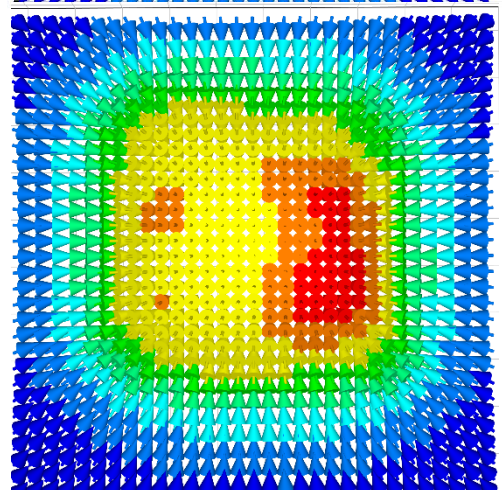
center



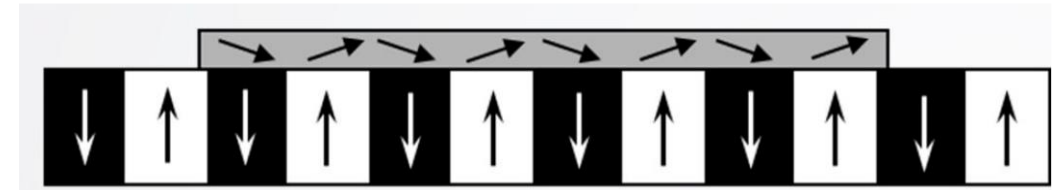
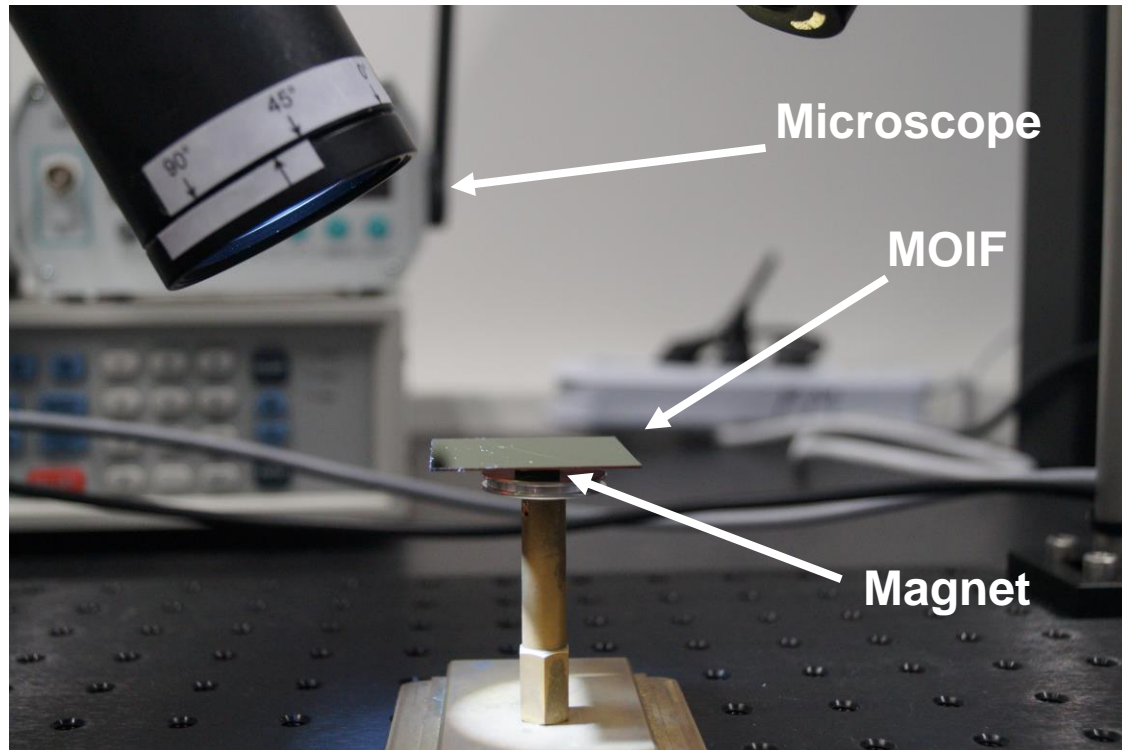
90% H_c



110% H_c



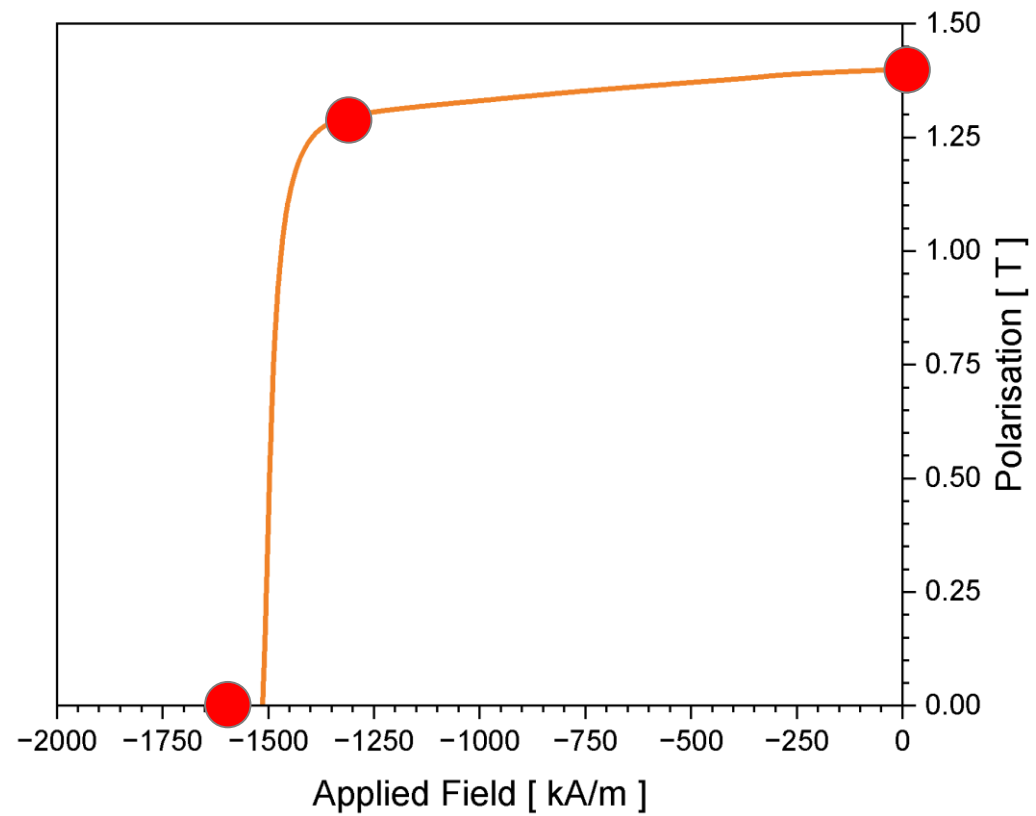
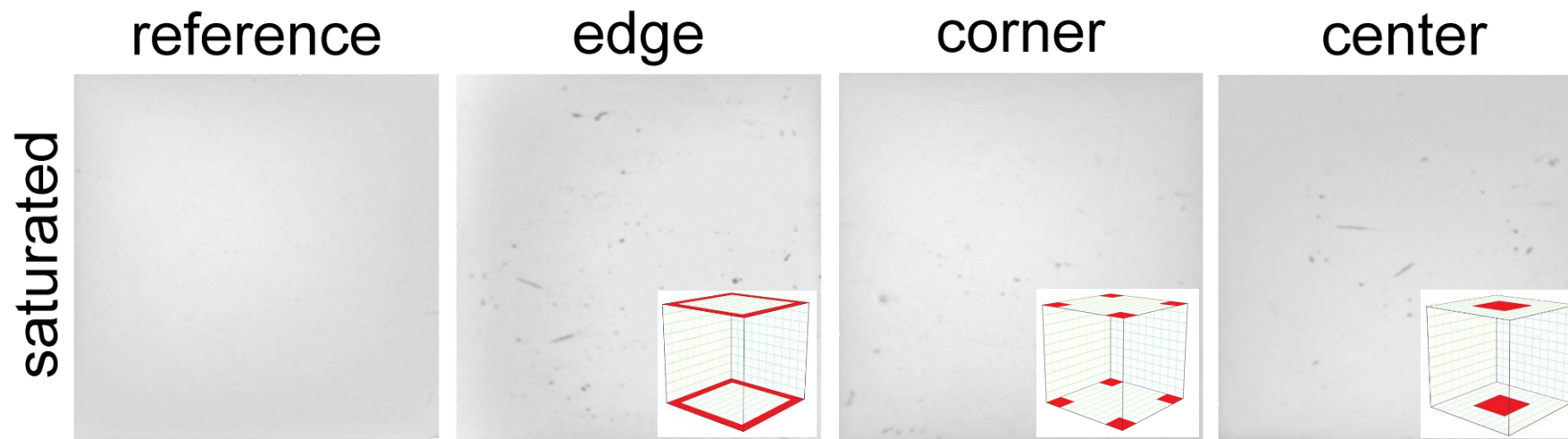
MOIF - Magneto-Optical Indicator Films

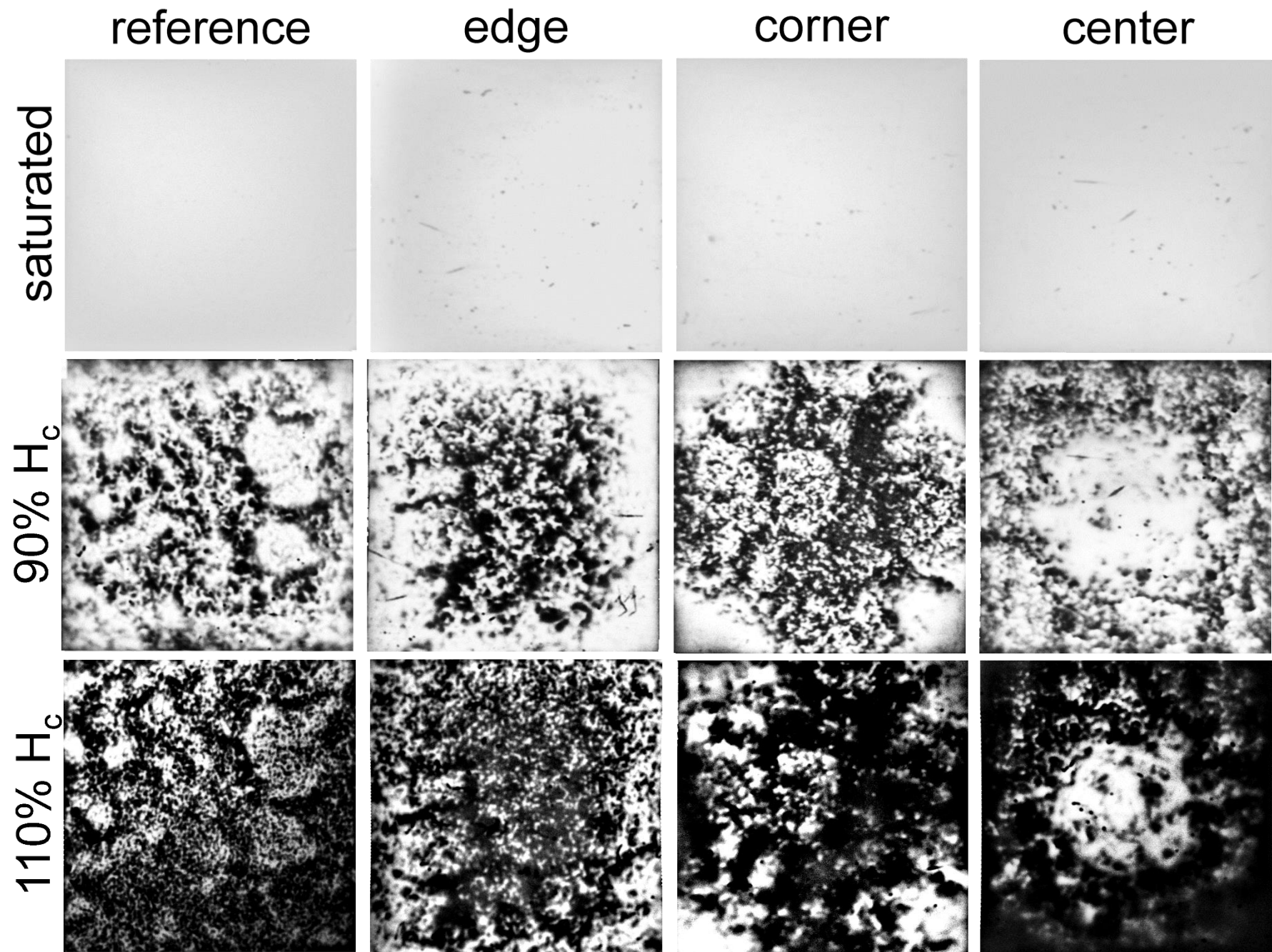


Rotation of magnetization in MOIF under the effect of the sample's stray field

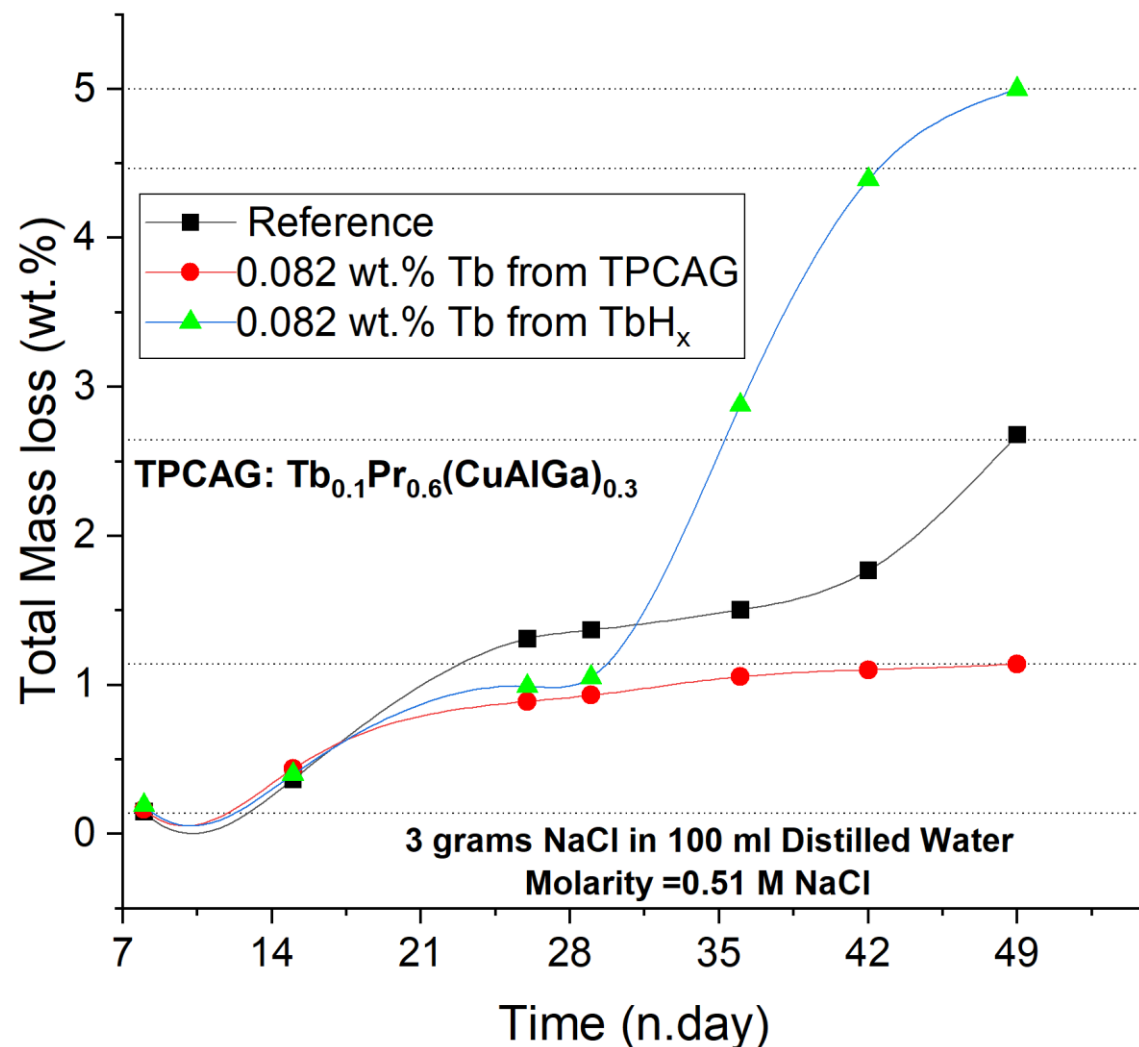
Magneto-optical contrast arises due to the Faraday effect

MOIFs as a tool for direct studies of the spatial distribution of magnetic fields and demagnetization processes in permanent magnets. High spatial resolution, large image range.





Corrosion: Tb-Pr-Al-Cu-Ga vs TbH_x



- Improved corrosion resistance for the Tb₁₀Pr₆₀(AlCuGa)₃₀ GBDP compared to reference magnet and TbH_x GBDP
- Confirmed also after 1 year air exposure

Tb₁₀Pr₆₀(AlCuGa)₃₀



TbH_x



After 1 year

Summary

- Low melting Tb-Pr-Al-Cu-Ga alloys are promising for GBDP
- HRE utilization drops significantly with increased GBDP amount
- **0.3 wt.% Tb:** $J_r = 1.4$ T, $H_c = 1990$ kA/m (2.5 T) & $H_c = 747$ kA/m (0.94 T) @ 150 °C
- Efficient Tb utilization via selected area GBDP
- Simple characterization using MOIF and 3D Hall scanner demonstrated
- Improved **corrosion resistance** compared to TbH_x and base magnet

